

Computational models for reinforced concrete slab systems

Autor(en): **Hinton, E. / Abdel Rahman, H.H. / Zienkiewicz, O.C.**

Objektyp: **Article**

Zeitschrift: **IABSE reports of the working commissions = Rapports des commissions de travail AIPC = IVBH Berichte der Arbeitskommissionen**

Band (Jahr): **34 (1981)**

PDF erstellt am: **10.07.2024**

Persistenter Link: <https://doi.org/10.5169/seals-26897>

Nutzungsbedingungen

Die ETH-Bibliothek ist Anbieterin der digitalisierten Zeitschriften. Sie besitzt keine Urheberrechte an den Inhalten der Zeitschriften. Die Rechte liegen in der Regel bei den Herausgebern.

Die auf der Plattform e-periodica veröffentlichten Dokumente stehen für nicht-kommerzielle Zwecke in Lehre und Forschung sowie für die private Nutzung frei zur Verfügung. Einzelne Dateien oder Ausdrucke aus diesem Angebot können zusammen mit diesen Nutzungsbedingungen und den korrekten Herkunftsbezeichnungen weitergegeben werden.

Das Veröffentlichen von Bildern in Print- und Online-Publikationen ist nur mit vorheriger Genehmigung der Rechteinhaber erlaubt. Die systematische Speicherung von Teilen des elektronischen Angebots auf anderen Servern bedarf ebenfalls des schriftlichen Einverständnisses der Rechteinhaber.

Haftungsausschluss

Alle Angaben erfolgen ohne Gewähr für Vollständigkeit oder Richtigkeit. Es wird keine Haftung übernommen für Schäden durch die Verwendung von Informationen aus diesem Online-Angebot oder durch das Fehlen von Informationen. Dies gilt auch für Inhalte Dritter, die über dieses Angebot zugänglich sind.



Computational Models for Reinforced Concrete Slab Systems

Modèles de calcul par ordinateur pour des systèmes de dalles en béton armé

Rechenmodelle für Stahlbetonplattensysteme

E. HINTON

Lecturer

Department of Civil Engineering, University College of Swansea,
Swansea, Wales, United Kingdom.

H.H. ABDEL RAHMAN

Research Assistant

O.C. ZIENKIEWICZ

Professor

SUMMARY

This paper discusses the finite element computational models used in program PLASAN for the nonlinear analysis of reinforced concrete slab systems. A layered Mindlin plate model is adopted and the discretisation is based on quadrilateral Mindlin elements. Some examples are presented and the relative efficiency of various nonlinear solution schemes is highlighted.

RÉSUMÉ

Dans cette publication on discute des modèles de calcul par la méthode des éléments finis, qui sont utilisés dans le programme PLASAN pour l'analyse non-linéaire des systèmes de dalles en béton armé. Un modèle de dalle multicouche MINDLIN est accepté et est basé sur des éléments MINDLIN quadrilatéraux. Certains exemples sont présentés et l'efficacité relative de différents schémas de solutions non-linéaires sont mises en valeur.

ZUSAMMENFASSUNG

Dieser Beitrag behandelt die Finite-Elemente-Rechenmodelle, die im Programm PLASAN für die nichtlineare Berechnung von Stahlbetonplatten verwendet werden. Ein Mindlin-Schichtplattenmodell wurde angenommen, während die Diskretisierung auf viereckigen Mindlin-Elementen beruht. Einige Beispiele werden gezeigt, und die relative Leistungsfähigkeit von verschiedenen nichtlinearen Lösungswegen wird beleuchtet.



1. INTRODUCTION

The present studies are motivated by the need to develop finite element computational models suitable for the accurate and efficient nonlinear analysis of reinforced concrete bridge decks and other flexural systems. Research work sponsored by the Highway Engineering Computer Branch (HECB) of the Department of Transport has resulted in the development of the computer program PLASAN [1]. This paper discusses the general approach in PLASAN and highlights the discretisation and equation solving techniques adopted therein. Results of some numerical experiments are also presented.

The present formulation is based on a layered reinforced concrete Mindlin plate model in which the plate is represented as a series of concrete and smeared unidirectional steel layers. Nonlinearities due to cracking, yielding and crushing of the concrete and yielding of the steel are taken into account. In PLASAN, the discretisation is based on a selectively integrated Heterosis quadrilateral plate element [2]. Experiments (not reported here) have been performed on other Mindlin elements. Two other useful elements emerge: a new 4-noded quadrilateral element developed recently by Hughes [3] and the 16-noded selectively integrated quadrilateral element [4]. Only the results obtained using the Heterosis element are discussed in this paper.

An accurate, reliable and efficient solution algorithm is of vital importance for the nonlinear analysis of reinforced concrete structures where cracking of the concrete forms a major problem. Although an elaborate modelling of the behaviour of the concrete and steel is essential, the solution algorithm plays an important role in the production of accurate results. In PLASAN, various incremental-iterative solution schemes are adopted. In the standard Newton-Raphson method (NR) the Jacobian (tangential stiffness matrix) is evaluated at each iteration. In the related methods various approximations to the Jacobian are used. In the Modified Newton-Raphson (MNR) methods, the approximation is updated only once for each increment and not for each iteration. Here the tangential stiffness matrix is formed and factored either at the beginning of each increment (KT1) or at the second iteration (KT2). Alternatively, the initial elastic stiffness matrix may be used throughout the entire analysis. This is known as the initial stress method (KO). Unfortunately NR and MNR methods have a tendency to diverge during elastic unloading and they sometimes lead to singular or ill-conditioned matrices near the limit load. The initial stress method provides a suitable solution to these problems but the convergence is slow particularly when fine convergence tolerances are used. The use of coarser tolerances with KO leads to faster convergence but at the expense of accuracy. Alternative computational strategies based on Quasi-Newton (QN) methods [5-7] offer a reasonable solution to this difficulty. In the present work, the BFGS Quasi-Newton updates are performed with the initial stiffness matrix (QNKO) and also in conjunction with MNR methods (QNKT1 and QNKT2). Line searches are also included in the MNR and QN methods. Various Secant Newton [8] and arc length methods [8-10] are also incorporated in PLASAN.

2. MINDLIN FORMULATION

In the usual Mindlin plate formulation the main assumption is that normals to the plate midsurface (xy -plane) before deformation remain straight but not necessarily normal to the midsurface after deformation. Thus the displacements u , v and w at any point with coordinates (x,y,z) can be expressed as

$$\begin{bmatrix} u(x,y,z) \\ v(x,y,z) \\ w(x,y,z) \end{bmatrix} = \begin{bmatrix} u_0(x,y) - z\theta_x(x,y) \\ v_0(x,y) - z\theta_y(x,y) \\ w_0(x,y) \end{bmatrix} \quad (1)$$

where u_0 , v_0 and w_0 are the displacements at the plate midsurface in the x , y and z direction and θ_x and θ_y are the rotations of the normal in the xz and yz plane respectively. Table I shows the main features of the Mindlin formulation.

3. MATERIAL MODEL

3.1 Concrete in compression

When failure is dominated by concrete cracking and steel yielding, a relatively crude plasticity model suffices. In PLASAN, the concrete is treated as an elasto-plastic material. In biaxial compression the Von Mises ellipse is used to define the elastic limit and the flow function. After yielding, the concrete is assumed to be crushed and lose all of its strength when the failure envelope (in strain space) is exceeded.

3.2 Concrete in tension

Cracks are assumed to open perpendicular to the higher principal stress direction when the tensile strength of concrete is exceeded. The stress level in the cracked concrete is interpolated using a tension stiffening curve and depends on the degree of straining in the concrete. Concrete cracked in two directions is assumed to lose all of its strength.

3.3 Steel reinforcement representation

In the uniaxial stress-strain relationship for the reinforcement steel a plasticity formulation is adopted in which linear isotropic strain hardening is assumed after initial yielding. Elastic unloading is allowed.

4. DISCRETISATION

The selectively integrated, 8-9 noded Heterosis element is used in the discretisation. In PLASAN, a hierarchical formulation is adopted to represent all degrees of freedom. Thus for typical element e , $N_1^{(e)}$ to $N_8^{(e)}$ are the 8-node Serendipity shape functions and $N_9^{(e)}$ is the bubble function $(1-\xi^2)(1-\eta^2)$ associated with the ninth central node. Thus the hierarchical degrees of freedom at node 9 are perturbations from the associated Serendipity interpolants. The 8-node Serendipity representation can be obtained if all degrees of freedom at node 9 are constrained to zero. If they are left free then an element equivalent to the 9-node Lagrangian representation is obtained. For the Heterosis representation, only the hierarchical lateral displacement at node 9 is restrained to zero. In this element selective integration procedures are adopted [2]. Unlike most other Mindlin elements, the Heterosis element is free from major defects. It does not give over stiff solutions in limiting thin plate situations (lock) nor does it have any transmittable mechanisms. The only other Mindlin elements which are considered worthy of further attention are the recently developed 4-noded quadrilateral [3] and the 16-noded quadrilateral [4]. Both of these elements have been successfully implemented within the present



Table I Mindlin plate formulation

Virtual work equation

$$\int_V \delta \underline{\epsilon}_1^T \underline{\sigma}_1 dV + \int_V \delta \underline{\epsilon}_2^T \underline{\sigma}_2 dV - \int_V \delta \underline{u}^T \underline{b} dV - \int_{S_t} \delta \underline{u}^T \underline{t} dS = 0$$

where

displacements $\underline{u} = [u, v, w]^T$	virtual displacement $\delta \underline{u} = [\delta u, \delta v, \delta w]^T$
in-plane strains $\underline{\epsilon}_1 = [u_{,x}, v_{,y}, u_{,y} + v_{,x}]^T$	$\delta \underline{\epsilon}_1 = [\delta u_{,x}, \delta v_{,y}, \delta u_{,y} + \delta v_{,x}]^T$
shear strains $\underline{\epsilon}_2 = [w_{,x} - \theta_{x1}, w_{,y} - \theta_{y1}]^T$	$\delta \underline{\epsilon}_2 = [\delta w_{,x} - \delta \theta_{x1}, \delta w_{,y} - \delta \theta_{y1}]^T$
in-plane stresses $\underline{\sigma}_1 = [\sigma_x, \sigma_y, \tau_{xy}]^T$	$\delta \underline{\sigma}_1 = [\delta \sigma_x, \delta \sigma_y, \delta \tau_{xy}]^T$
shear stresses $\underline{\sigma}_2 = [\tau_{xz}, \tau_{yz}]^T$	$\delta \underline{\sigma}_2 = [\delta \tau_{xz}, \delta \tau_{yz}]^T$

Incremental stress/strain relationships

$$d\underline{\sigma}_1 = \underline{D}_1 d\underline{\epsilon}_1$$

$$d\underline{\sigma}_2 = \underline{D}_2 d\underline{\epsilon}_2$$

Elastic

$$\underline{D}_1 = \underline{D} = \frac{E}{(1-\nu^2)} \begin{bmatrix} 1 & \nu & 0 \\ \nu & 1 & 0 \\ 0 & 0 & \frac{1-\nu}{2} \end{bmatrix}$$

$$\underline{D}_2 = \frac{E}{2(1+\nu)\alpha} \begin{bmatrix} 1 & 0 \\ 0 & 1 \end{bmatrix}$$

α is a modification factor (usually $\alpha = 1.2$)

Plastic

$$\underline{D}_1 = \underline{D} - \underline{D} \begin{bmatrix} \partial F \\ \partial \underline{\sigma}_1 \end{bmatrix} \begin{bmatrix} \partial F \\ \partial \underline{\sigma}_1 \end{bmatrix}^T \underline{D} \left[\bar{A} + \frac{\partial F}{\partial \underline{\sigma}_1} \underline{D} \frac{\partial F}{\partial \underline{\sigma}_1} \right]^{-1}$$

in which F is the yield function

$$F = F(\underline{\sigma}_1, H) \quad \bar{A} = -\frac{1}{\lambda} \frac{\partial F}{\partial H}$$

λ is the proportionality constraint

H is the hardening parameter

Finite element discretization

$$\underline{u} = \sum_i N_i \underline{a}_i$$

$$\underline{\epsilon}_1 = \sum_i B_{1i} \underline{a}_i$$

$$\underline{\epsilon}_2 = \sum_i B_{2i} \underline{a}_i$$

where $N_i = N_i \begin{bmatrix} 1 & 0 & 0 & -z \\ 0 & 1 & 0 & 0 \\ 0 & 0 & 1 & 0 \\ 0 & 0 & 0 & -z \end{bmatrix}$

$$\underline{a}_i = [u_i, v_i, w_i, \theta_{x1}, \theta_{y1}]^T$$

$$B_{1i} = \begin{bmatrix} N_{i,x} & 0 & 0 & -zN_{i,x} & 0 \\ 0 & N_{i,y} & 0 & 0 & -zN_{i,y} \\ N_{i,y} & N_{i,x} & 0 & -zN_{i,y} & -zN_{i,x} \end{bmatrix} \quad B_{2i} = \begin{bmatrix} 0 & 0 & N_{i,x} & -N_i & 0 \\ 0 & 0 & N_{i,y} & 0 & -N_i \end{bmatrix}$$

Stiffness Matrices

$$K_{ij} = \int_V B_{1i}^T \underline{D}_1 B_{1j} dV + \int_V B_{2i}^T \underline{D}_2 B_{2j} dV$$

Residual forces

$$\underline{\Psi}_i = \int_V B_{1i}^T \underline{\sigma}_1 dV + \int_V B_{2i}^T \underline{\sigma}_2 dV - \underline{f}_i$$

where the consistent nodal forces $\underline{f}_i = \int_V N_i^T \underline{b} dV + \int_{S_t} N_i^T \underline{t} dS$



framework but results are not reported here.

5. SOLUTION SCHEMES

5.1 Standard and modified Newton-Raphson methods

Various incremental-iterative solution schemes are incorporated in PLASAN. In all of the methods the aim is to reduce the residual forces to small values. The residual force may be expressed as

$$\underline{\psi}(\underline{d}_i) = \int_V \underline{B}_{1i}^T \underline{\sigma}_{1i} dv + \int_V \underline{B}_{2i}^T \underline{\sigma}_{2i} dv - \underline{f}_i \quad (2)$$

where $\underline{f}_i = \lambda_i \underline{f}$ is the applied load vector and λ_i , \underline{d}_i , \underline{B}_{1i} , \underline{B}_{2i} , $\underline{\sigma}_{1i}$ and $\underline{\sigma}_{2i}$ are the loading parameter, displacement vector and strain-displacement matrices and stress vectors respectively. The vector \underline{f} is a reference load vector and subscripts 1 and 2 refer to inplane and transverse shear quantities respectively.

In incremental-iterative solution schemes a sequence of corrections $\delta \underline{d}_i$ to the displacement vector are produced. Using the expression

$$\delta \underline{d}_i = - [\underline{K}_i]^{-1} \underline{\psi}_i \quad (3)$$

where \underline{K}_i is an approximation to the Jacobian matrix which may be expressed as

$$\underline{J}(\underline{d}_i) = \left. \frac{\partial \underline{\psi}_i}{\partial \underline{d}} \right|_{\underline{d}=\underline{d}_i} \quad (4)$$

The new estimate to the displacement vector is then given as

$$\underline{d}_{i+1} = \underline{d}_i + \eta_i \delta \underline{d}_i \quad (5)$$

where η_i may be found from a line search along direction $\delta \underline{d}_i$ which satisfies the condition

$$|[\delta \underline{d}_i]^T \underline{\psi}_{i+1}| \leq 0.5 |[\delta \underline{d}_i]^T \underline{\psi}_i| \quad (6)$$

where $\underline{\psi}_{i+1}$ is found using the estimate \underline{d}_{i+1} . Often no line search is performed and η_i is taken as unity.

Various solution schemes are implemented in PLASAN using different approximation to the Jacobian matrix:

- KO \underline{K}_i is the initial elastic stiffness matrix
- NR $\underline{K}_i = \underline{J}(\underline{d}_i)$
- KT1 $\underline{K}_i = \underline{J}(\underline{d}_i)$
- KT2 for $i > 1$, $\underline{K}_i = \underline{J}(\underline{d}_i)$

5.2 Quasi-Newton BFGS Methods

In PLASAN various Quasi-Newton BFGS methods are adopted in the form given by Matthies and Strang [5]. These methods seek to satisfy the secant condition

$$\underline{K}_i (\underline{d}_i - \underline{d}_{i-1}) = \underline{\psi}_i - \underline{\psi}_{i-1} \quad (7)$$



The BFGS update which does not destroy the banded nature of the stiffness matrix is given in the form

$$\underline{K}_i^{-1} = \{ \underline{I} + \underline{w}_i \underline{v}_i^T \} [\underline{K}_{i-1}]^{-1} \{ \underline{I} + \underline{v}_i \underline{w}_i^T \} \quad (8)$$

where

$$\underline{v}_i = \underline{\psi}_{i-1} \left\{ 1 + \left[\frac{n_{i-1} \delta \underline{d}_{i-1}^T \underline{\gamma}_i}{\delta \underline{d}_{i-1}^T \underline{\psi}_{i-1}} \right]^{\frac{1}{2}} \right\} - \underline{\psi}_i$$

$$\underline{w}_i = \delta \underline{d}_{i-1} / (\delta \underline{d}_{i-1}^T \underline{\gamma}_i)$$

and

$$\underline{\gamma}_i = \underline{\psi}_i - \underline{\psi}_{i-1}$$

Equation (8) may be expanded and written in the form

$$\underline{K}_i^{-1} = \left[\prod_{j=i-1}^1 \{ \underline{I} + \underline{w}_j \underline{v}_j^T \} \right] \underline{K}_1^{-1} \left[\prod_{j=1}^{i-1} \{ \underline{I} + \underline{v}_j \underline{w}_j^T \} \right] \quad (9)$$

In PLASAN the following variations are available

- QNKO \underline{K}_1 is the initial elastic stiffness matrix
- QNKT1 $\underline{K}_1 = \underline{J}(\underline{d}_1)$
- QNKT2 $\underline{K}_1 = \underline{J}(\underline{d}_2)$

Thus in QNKT2 the updates begin after the first iteration.

Crisfield [8] has suggested various Secant-Newton (SN) methods. In one of these equation (8) is used and \underline{K}_{i-1} is always taken as $\underline{J}(\underline{d}_1)$. A major attraction of this method is that no previous values of \underline{v}_i and \underline{w}_i need be stored.

5.3 Arc length methods

Recently arc length methods have gained much popularity due to their ability to deal with geometrically nonlinear problems involving snap-through and snap-back behaviour [8-10]. The normal plane (NP) and spherical path (SP) variants are both implemented in PLASAN. In the normal plane method within a given increment the solution is constrained to lie in a plane normal to the tangent to the equilibrium curve at the beginning of the increment. In the spherical path method the solution is constrained to lie on a sphere of radius equal to the arc length which is defined as

$$\ell = [\Delta \underline{d}_1^T \Delta \underline{d}_1 + (\Delta \lambda_1)^2 \underline{f}^T \underline{f}]^{\frac{1}{2}} \quad (10)$$

In both the NP and SP methods it is necessary to evaluate updates $\delta \lambda_i$ which adjust the total load level for the increment. The arc length may be updated from increment to increment and Ramm [9] suggests the use of the equation in which the current arc length at load step n is given as

$$\ell^{(n)} = \ell^{(n-1)} (I_D / I^{(n-1)})^{\frac{1}{2}} \quad (11)$$

where I_D is the desired number of iterations per load step and $I^{(n-1)}$ is the actual number of iterations required in the previous load step. Further details of the methods are given elsewhere [8-10].



5.4 Convergence and final failure

Displacement, residual force and energy norms are used to check convergence in PLASAN. Final failure is assumed to occur when the current stiffness parameter [11] (which is a parameter that characterizes the overall stiffness of the slab) is less than some specified value.

Table II Solution time comparisons for Mueller slab

ALGORITHM	CPU		
	1.0%	0.1%	0.01%
K _O	41	123*	73*
NR	67	88*	146*
KT1	35 (34)	79* (71)	101* (109)
KT2	30 (35)	37* (45)	46* (61)
QNKO	29	49	64
QNKT1	32 (35)	37 (52)	44 (66)
QNKT2	32 (35)	34 (41)	42 (59)

* Failed to converge after 50 iterations

() Values with line search

* Premature structure failure



6. EXAMPLES

6.1 Mueller slab

This section is devoted to a comparison of different solution schemes for reinforced concrete plates. All methods are implemented in the same computer program so that all tasks - apart from those peculiar to the particular algorithm adopted - are accomplished in exactly the same way.

A corner supported doubly reinforced concrete slab tested by Mueller [12] is analysed using a 3x3 mesh in a symmetric quadrant. Numerical experiments are then carried out to test the accuracy and efficiency of the different solution algorithms suggested in this paper. Large load increments have been used and only 6 nonlinear increments are required. A summary of the results is given in Table II, while the load-central deflection curves of the slab are given in Figure 1. A study of the results shows that the use of KO with a coarse convergence tolerance (1.0%) results in over-stiff behaviour in the final stages of loading and an overestimation of the failure load. The rest of the algorithms, when they work, predict practically the same displacements regardless of the convergence tolerance used ($\leq 1.0\%$). However, it should be noticed that the convergence of the solution when KO is adopted is very slow and that the solution fails to converge within the specified number of iterations at a lower load level when a tighter convergence tolerance is used. Newton-Raphson and Modified Newton-Raphson - KT2 - methods indicate premature failure when fine convergence tolerances are used. The convergence of KT1 is also very slow at the later stages of loading. However when line searches are used with these methods reliable solutions are obtained. Methods based on BFGS updates always converge to the required convergence tolerance at a minimum cost. The use of BFGS updates with KO and a convergence tolerance of 1% renders the cheapest analysis for this slab and also retains all the advantages of using KO such as the possibility of elastic unloading, etc. If a finer convergence tolerance is required the BFGS - KT2 algorithm may be chosen. In the present example, the tension stiffening effect of reinforced concrete is exploited and on cracking the concrete is only allowed to release its tensile stresses gradually according to the tension stiffening curve shown in Figure 1. However, if the tension stiffening of reinforced concrete is not considered, or if only a small amount of stiffening is allowed, then the cracking of the concrete becomes severe resulting in large residual forces and the value under the square root in (8) may become negative preventing the use of the BFGS update. This situation occurred during another numerical experiment on a simply supported plate tested experimentally by Taylor et al [13]. Here a line search helps the BFGS updates to be applied and reduces the analysis cost considerably.

6.2 McNiece slab

Another numerical experiment is carried out using the well known corner supported McNiece slab [14] which has been tested numerically by many analysts. In this experiment a comparison is made between MNR, KT1 method and other methods used in conjunction with it, such as the Secant-Newton (SN2), the Quasi-Newton (QNKT1) and the spherical path (ARC-SP) methods. The automatic load incrementation is used first with the arc method, then the other techniques are used with the same prescribed increments. The displacement norm is used to check for convergence with a tolerance of 0.1%. The displacements predicted by the different techniques are almost identical and in good agreement with the experiment, see Figure 2. The cost of the analysis differs dramatically. In the KT1 method the solution fails to converge within the specified number of iterations and the Secant and Quasi-Newton methods do equally well. The superiority of the arc method in this problem is clear. However, it must be noted

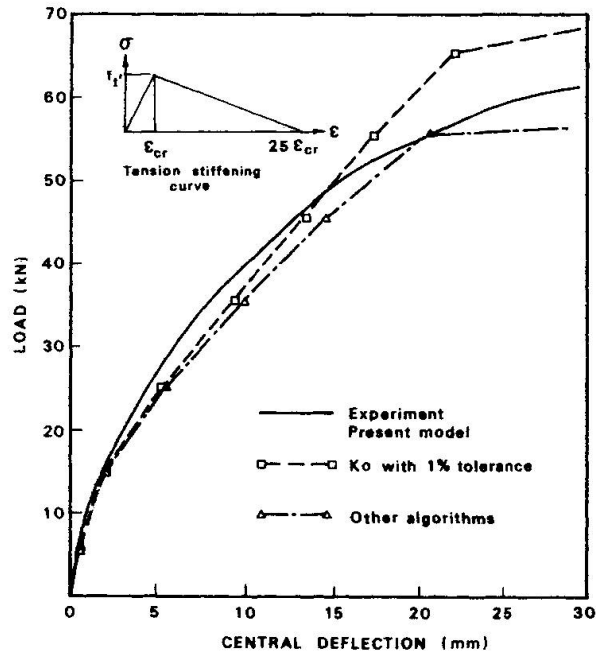


Figure 1 Load-central deflection curve for the Mueller slab

ALGORITHM.	KT1	QNKT1	SN2	ARC-SP
CPU	> 146	108	102	72

CPU TIME FOR DIFFERENT ALGORITHMS

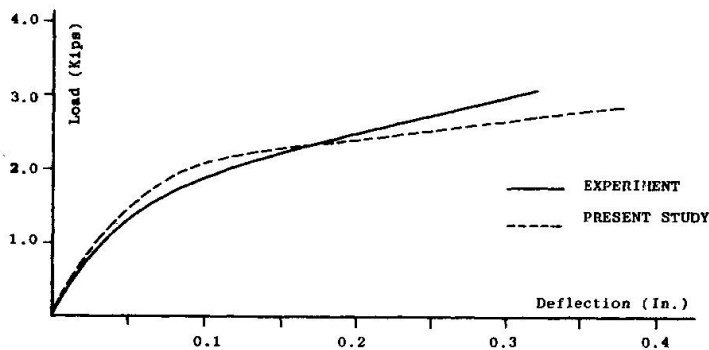
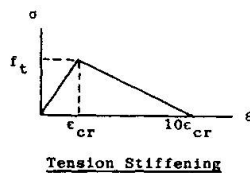


Figure 2 Load-central deflection curve for the McNeice slab and comparison of various algorithms



that when the tension stiffening effect of reinforced concrete after cracking is not fully exploited, and there is an instantaneous loss of strength, numerical difficulties may be anticipated. The use of line searches and relatively coarser convergence tolerances, together with some restart criteria to safeguard against divergence of solution, could be advantageous.

7. CONCLUSIONS

From the results discussed in the previous section and from other experience, it can be concluded that the use of the initial stress method in the nonlinear analysis of reinforced concrete plates with coarse convergence tolerances may result in an overestimation of the failure loads. The use of BFGS updates with the initial stiffness method, or Modified Newton-Raphson methods, is suggested for a reliable and relatively inexpensive nonlinear analysis of reinforced concrete plates if tension stiffening of concrete is considered. The use of line searches with methods based on BFGS updates is recommended if the tension stiffening of reinforced concrete is not considered. The arc length and Secant Newton methods also show promise.

REFERENCES

1. ABDEL RAHAMN, H. H. and HINTON, E.; "User manual for program - PLASAN", Report Dept. of Civil Eng., Swansea, June 1981.
2. HUGHES, T. J. R. and COHEN, M.; "The Heterosis finite element for plate bending", Computers and Structures, Vol. 9, 1978, pp.445-450.
3. HUGHES, T. J. R. and TEZDUYAR, T. E.; "Finite elements based upon Mindlin plate theory with particular reference to the four-node bilinear isoparametric element", to appear in J. Appl. Mech.
4. WONG, T. K.; "Nonlinear analysis of reinforced concrete slab systems using cubic Mindlin plate elements", M.Sc. Thesis, University College of Swansea, Jan. 1981.
5. MATTHIES, H. and STRANG, G.; "The solution of nonlinear finite element equations", Int. J. Num. Meth. in Engng., Vol. 14, 1979, pp.1613-1626.
6. BATHE, K. J. and CIMENTO, A.; "Some practical procedures for the solution of nonlinear finite element equations", Comp. Meth. in Appl. Mech. Eng., Vol. 22, 1979.
7. ENGELMAN, M. S., STRANG, G. and BATHE, K. J.; "An application of Quasi-Newton methods in fluid mechanics", to appear in Int. J. Num. Meth. in Engng., 1981.
8. CRISFIELD, M. A.; "Incremental/iterative solution procedures for nonlinear structural analysis", Proceedings of the Int. Conf. on Numerical Methods for Nonlinear Problems, University College of Swansea, Pineridge Press, 1980, pp.261-290.
9. RAMM, E.; "Strategies for tracing nonlinear response near limit points", Institut für Baustatik der Universität Stuttgart, W. Germany, 1980.
10. HINTON, E. and LO, C. S.; "Large deflection analysis of imperfect Mindlin plates using the modified Riks method", MAFELAP 1981, May, 1981. Proceedings to be published by Academic Press.



11. BERGAN, P. G.; "Solution algorithms for nonlinear structural problems", Computers and Structures, Vol. 12, 1980, pp.497-509.
12. MUELLER, G.; "Numerical problems in nonlinear analysis of reinforced concrete", UC-SESM Report No. 77-5, University of California, Sept. 1977.
13. TAYLOR, R., MAHER, D. R. H. and HAYES, B.; "Effect of the arrangement of reinforcement on the behaviour of reinforced concrete slabs", Magazine of Concrete Research, Vol. 18, No. 55, June 1966, pp.85-94.
14. JOFRIET, J. C. and McNIECE, G. M.; "Finite element analysis of reinforced concrete slabs", J. Struct. Division, ASCE, Vol. 97, No. ST3, 1971, pp.785-807.

Leere Seite
Blank page
Page vide